The University of Chicago

Center for EPR Imaging In Vivo Physiology

High Spatial and Spectral Resolution Electron Spin Echo Oxygen Imaging (ESEOI) using Bandwidth- Extended Electron Paramagnetic Resonance Imaging (EPRI) at Low Frequencies

Payam Seifi; Boris Epel; Subramanian V. Sundramoorthy; Colin Mailer and Howard J. Halpern

Department of Radiation and Cellular Oncology, Center for EPR Imaging In Vivo Physiology, University of Chicago, Chicago, IL 60637

Introduction

The knowledge of local partial oxygen pressure (pO2) in malignant tumors is important due to the effect of hypoxia, or low oxygen concentration, on tumor aggressiveness and response to radiation therapy. Three dimensional ESEOI is an exciting new means to provide a quantitative, spatially resolved measure of pO_2 inside a tumor [1,2] (Fig. 1). The Spatial resolution of the ESE image is defined in part by the gradient field magnitude and therefore is limited by the imager frequency bandwidth, which also limits the maximum object size that can be imaged. The bandwidth limitation can be avoided using multiple magnetic field (Multi-B) technique.

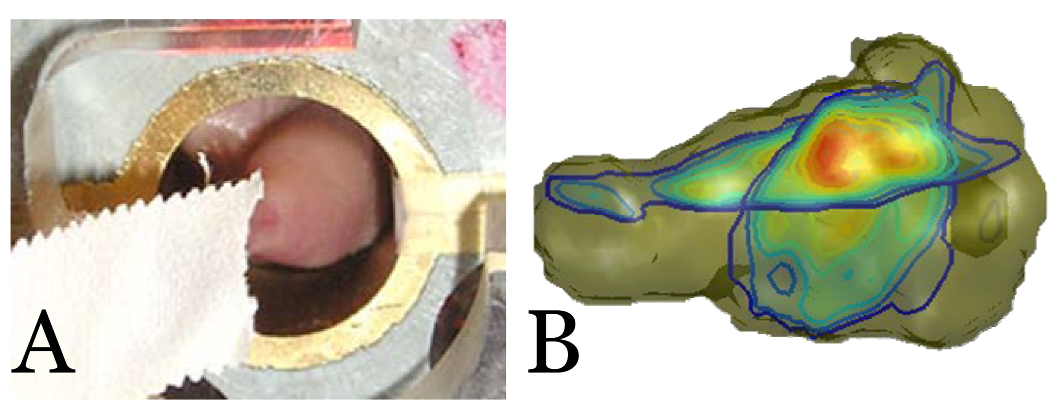

Figure 1.
(A) A tumor-bearing mouse leg placed in the loop-gap resonator for EPR imaging.
(B) A 3-D visualization of the resulting oxygen image.

Objectives

The goal is to extend the effective acquisition bandwidth of the imaging system using this Multi-B technique, apply magnetic field gradients up to 50mT/m, corresponding to spatial resolution of ~ 300µm, and image objects as large as 10cm in length which has relevance to human tumor size imaging.

Theoretical Background

Electron Spin Echo (ESE) is based on the interaction of unpaired electron spins with pulsed RF radiation in an otherwise uniform magnetic field, where spins are first rotated by the first pulse (excitation) and then focused again by the second pulse (refocusing) that rotates spins in the plane and generated echo signal (Fig. 2). Oxygen concentration in the tissue can be measured by how quickly the resulting echo signal decays (T_2). In order to encode information in the echo signal, gradients of magnetic field are used. Ideally, the output echo signal is proportional to Radon transform of the weighted spin distribution in the object. In practice, EPR absorption line blurs the projections, demanding larger gradients for high spatial resolution. Finite width of the acquisition window causes truncation in projection when large gradients are applied (for high resolution imaging) or large objects are imaged.

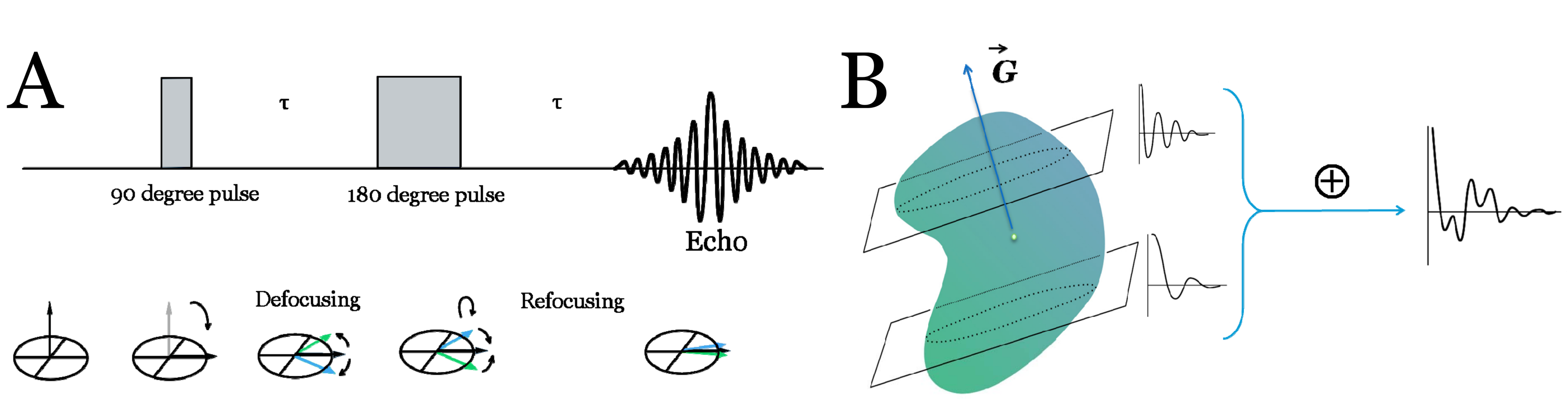

Figure 2.
(A) ESE spectroscopy principle, (B) Magnetic field gradients used for frequency encoding

Methods and Materials

The 3cm long by 1cm diameter sealed bottle phantom with two 1 mm capillary tube phantoms filled with spin probe OX063H [3] at 1mM concentration was employed to test the resolution performance of the Multi-B technique (fig. 3A). An 8.5cm long by 16mm diameter tube phantom filled with at 0.2mM spin probe concentration was employed for large object study (fig. 3B). Our pulse imager has approximately a 10MHz frequency bandwidth, sufficient to image a 2.0cm long sample using 15mT/m field gradient in the standard ESE technique (single-B) without any significant truncation errors. In the Multi-B technique, the experiment is repeated at several magnetic field offsets in order to increase the effective acquisition bandwidth.

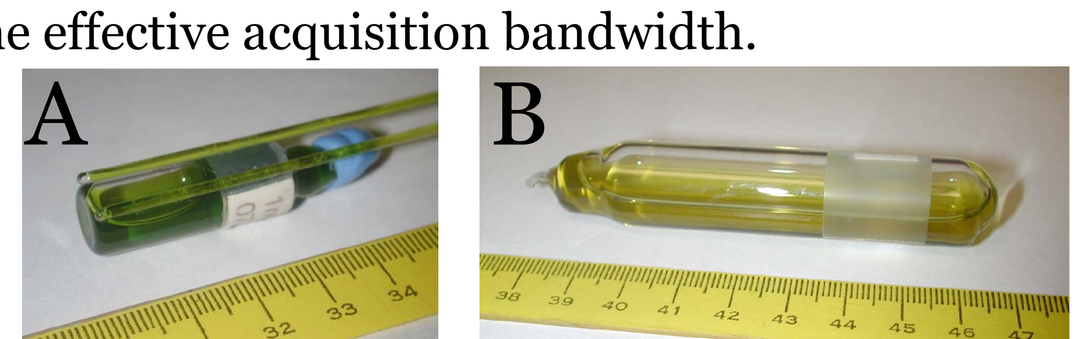

Figure 3.
(A) Resolution study phantom.
(B) Large Object Imaging phantom

Theoretical Model: $$S(\upsilon, \boldsymbol{G}) = \frac{P(\upsilon)}{\gamma|\boldsymbol{G}|} \cdot \tilde{s}_0(\upsilon) *_{\upsilon} Rad\left(\rho(\boldsymbol{r})e^{-\frac{2\tau}{T_2(\boldsymbol{r})}}; \hat{\boldsymbol{\alpha}}, \frac{\upsilon}{\gamma|\boldsymbol{G}|}\right)$$

The EPR absorption line-width acts as a point spread function (PSF). Increasing gradients reduces the blur effect. We want it to be **narrow**.

Radon transform of spin density map weighted with T_2 decay.

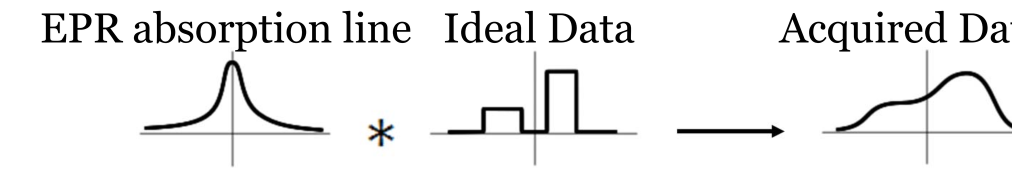

P(υ): The acquisition window function, which is a multiplicative term. Distortions may be corrected if they are small, otherwise it introduces truncation. We want it to be **wide**.

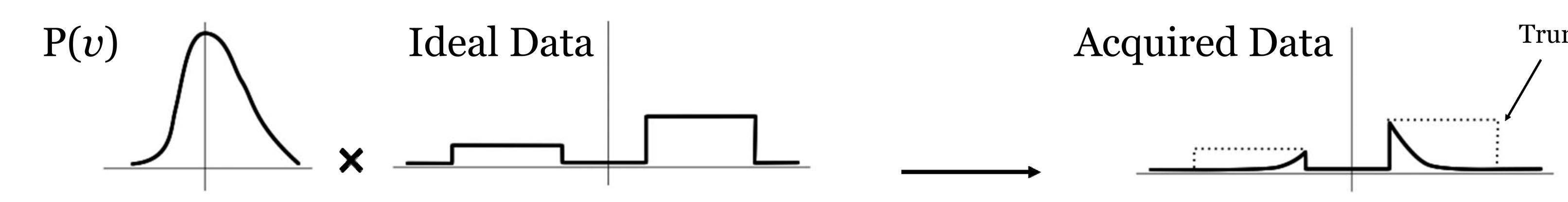

The Multi-B scheme provides extension of the effective acquisition window by repeating experiment at multiple main magnetic field offsets.

Single-B bandwidth: ~ 10 MHz

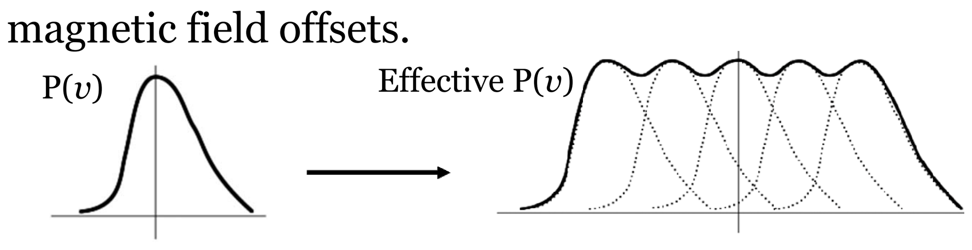

Multi-B bandwidth: > 25 MHz

Results

While at small gradients (low resolutions) Multi-B images resemble those from Single-B, at large applied gradients Multi-B images have better spatial and spectral (or T_2) resolutions (Table 1), and less image artifacts (fig. 4). Large object imaging previously impossible in conventional ESE can be done with the new technique (fig. 5). Comparing animal images with the same duration, those acquired using Multi-B have less image artifacts (fig. 6).

Table 1.
Measured spatial and T_2 resolution for Single- and Multi-B images with different gradients.

ESE Protocol Gradient	Spatial Resolution, FWHM (mm)				T_2 Resolution, standard deviation (µs)			
	15 mT/m	20 mT/m	25 mT/m	30 mT/m	15 mT/m	20 mT/m	25 mT/m	30 mT/m
ESE-Single-B	1.37 (0.08)	1.01 (0.10)	ND *	ND	0.33	0.51	ND	ND
ESE-Multi-B	1.03 (0.07)	0.88 (0.04)	0.78 (0.08)	0.75 (0.11)	0.39	0.38	0.47	0.53

* ND: Not Determines due to severe image truncation artifacts. See fig. 4.

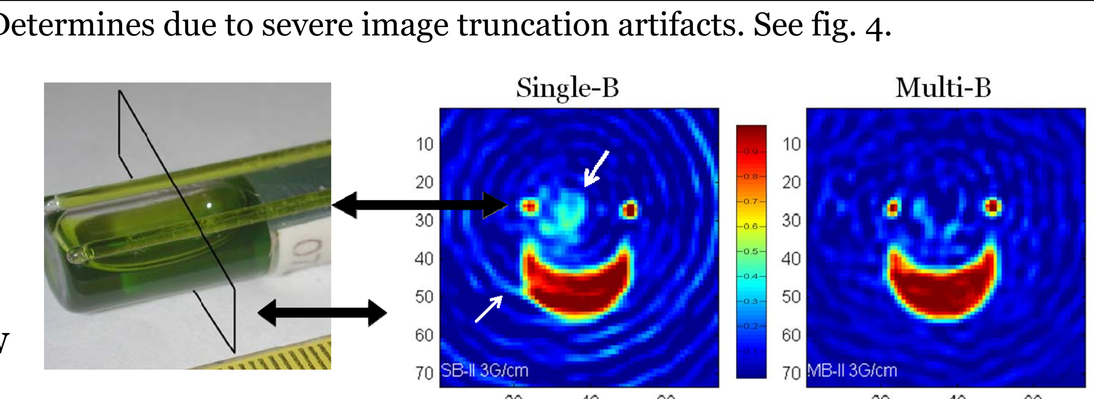

Figure 4.
Single-B vs. Multi-B comparison for high resolution imaging. (2D section of the 3D image shown.) Gradient: 30mG/m, Field of view (FOV): 25mm.

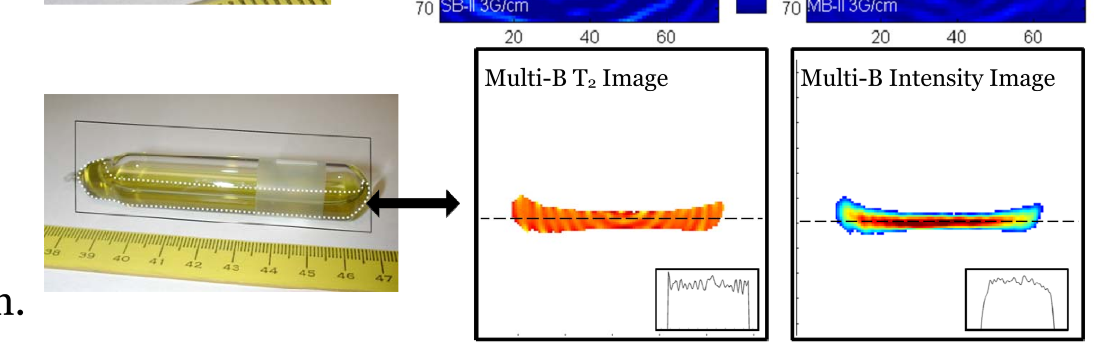

Figure 5.
Large object Multi-B imaging, showing 2D sections of the 3D T_2 and intensity images. FOV:11.3cm.

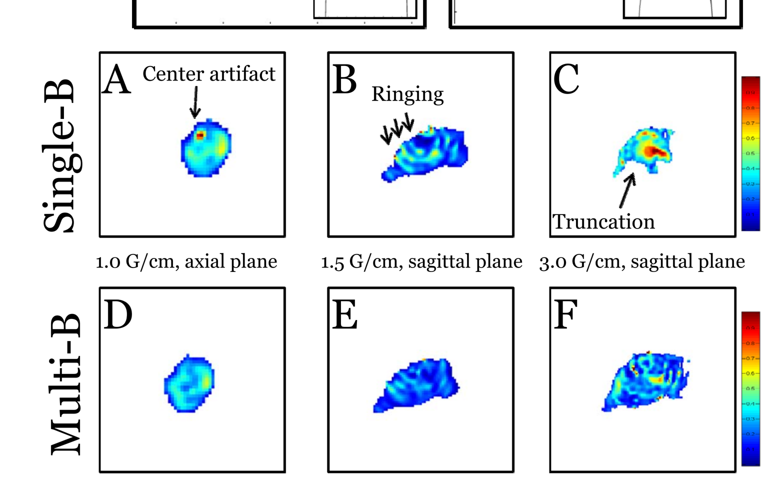

Figure 6.
Animal imaging showing cancellation of hole artifact (A,D), ringing artifacts (B, E) and truncation artifact (C, F) when switching from single-B to Multi-B images. Images are taken from C3H strain of mice having FSa tumor. FOV: 4.2cm.

Conclusions

The Multi-B method was found to be superior in overcoming the instrumental limitations in applying larger magnetic gradient fields, or obtaining images from larger objects with higher spatial resolution compared to standard ESE imaging techniques.

References

[1] Mailer C. *et al., Magn. Reson. In Medicine (2006),* **55, 904-912**

[2] Epel B. *et al., Concepts in Magn. Reson. B (2008)* **33B, 163 - 176**

[3] Elas M. *et al., Magn. Reson. In Medicine (2003),* **49, 682-691**.

Acknowledgements

Help for animal imaging was from E. Barth, B. Butler and C. Li. The work is supported by NIH grants P41-EB002034 and R01-CA98575.

Presented at 2nd Annual North American School of Information Theory, Evanston, IL, August 10-13, 2009.